Supplement of Biogeosciences, 23, 3323–3346, 2026
https://doi.org/10.5194/bg-23-3323-2026-supplement

Biogeosciences Open Access EGU

Supplement of

Marine carbonate system variability from tidal to seasonal timescales at the interface between the North Sea and Wadden Sea

Yasmina Ourradi et al.

Correspondence to: Yasmina Ourradi (yasmina.ourradi@nioz.nl)

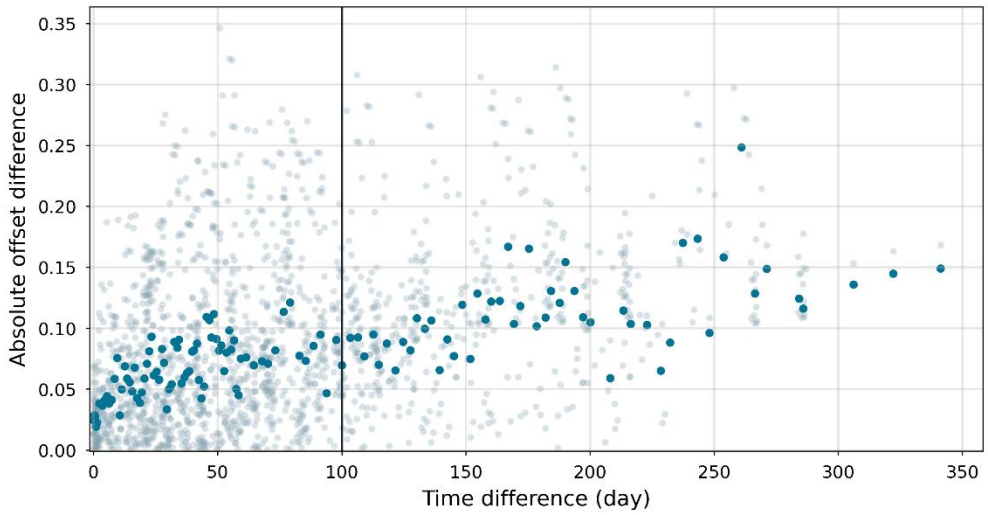

Figure S1. Semivariogram of the temporal variability of pH offset differences for the entire study period. Light grey points in the background represent all possible pairs of pH offset differences, while dark circles indicate the mean values calculated using moving bins.

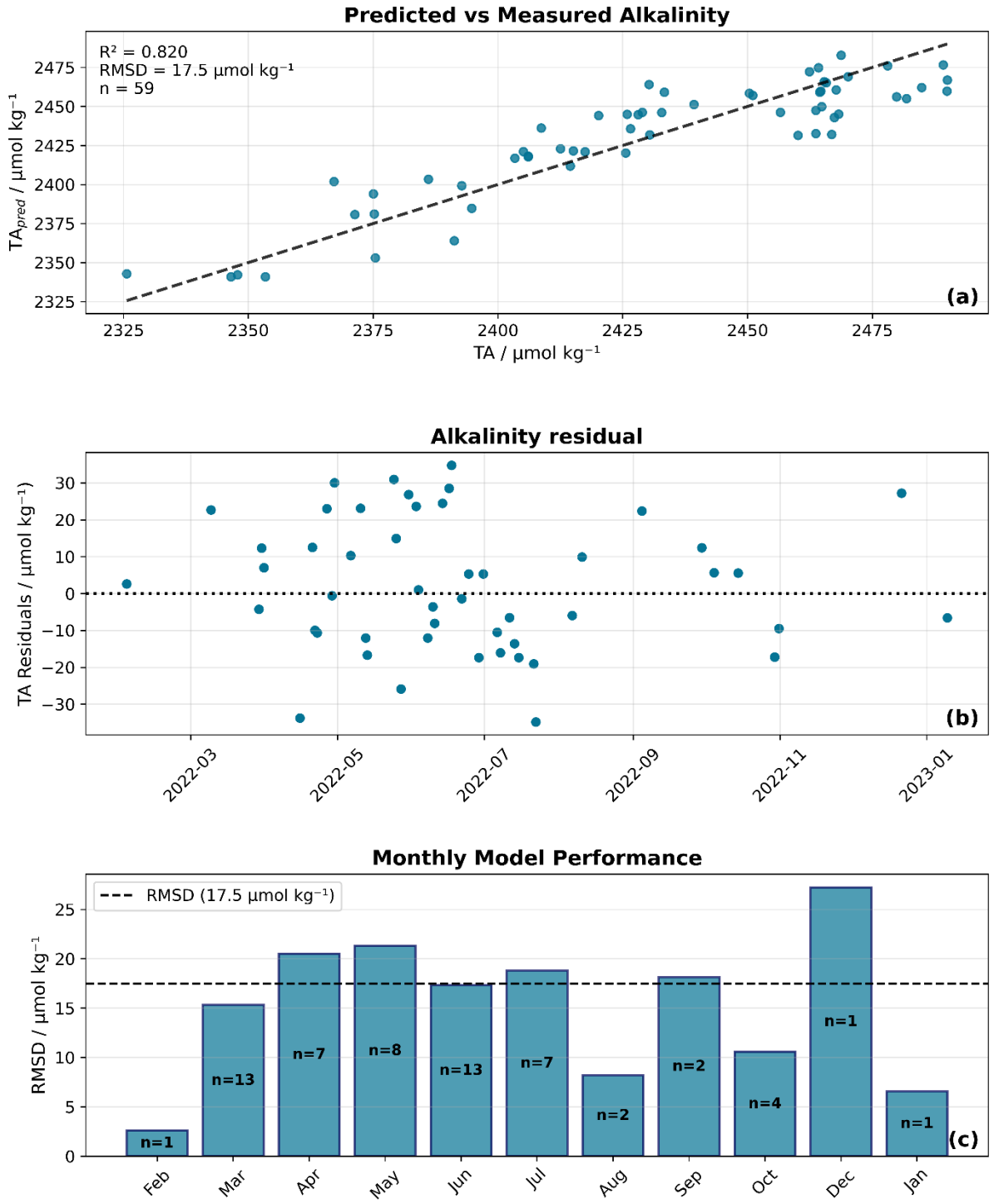

Figure S2. Model performance evaluation for TA predictions. (a) Shows predicted versus measured TA values, with the 1:1 line and statistical metrics, including coefficient of determination (R^2), root mean square deviation (RMSD), and sample size (n). **(b)** Time series of TA residuals (measured minus predicted values) showing temporal patterns in model performance, with the zero-line indicating perfect prediction (dotted black line). **(c)** Monthly model performance expressed as RMSD values. The horizontal dashed line indicates the overall RMSD across all months. Sample sizes (n) for each month are displayed within the bars.

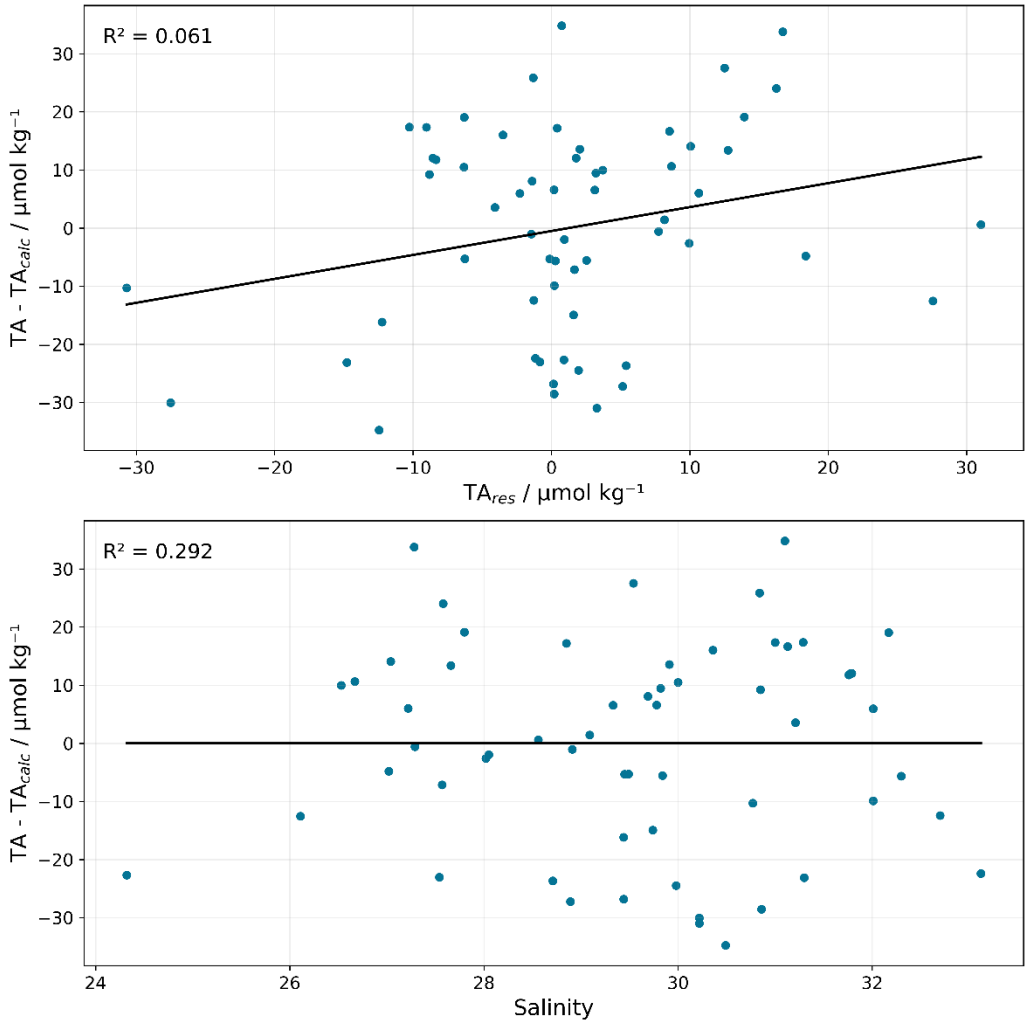

Figure S3. Relationship between TA_{res} and OrgAlk ($TA - TA_{calc}$) and salinity. **(a)** Correlation between $TA - TA_{calc}$ and TA_{res}, with linear regression line (black) and coefficient of determination (R^2). **(b)** Correlation between salinity and TA_{res}, with linear regression line (black) and R^2.

Figure S4. pH calibration approach on high-resolution DIC calculations during a 72-hour period.

In (a): DIC calculated from TA_{pred} and pH sensor data using different calibration strategies: blue line represents the DIC that was calculated suing pH calibrated with all available high-resolution pH samples. Red line represents the DIC calculated using pH recalibrated based on only two reference points indicated in red in (b). Black scatter points indicate all measured DIC.

In (b): Corresponding high-resolution pH time series. Black scatter points indicate all measured pH values. The blue line represents the calibrated pH using the full dataset and in red line the pH that was recalibrated using two selected calibration points shown in red in (b). Vertical dashed lines represent the daily boundaries.

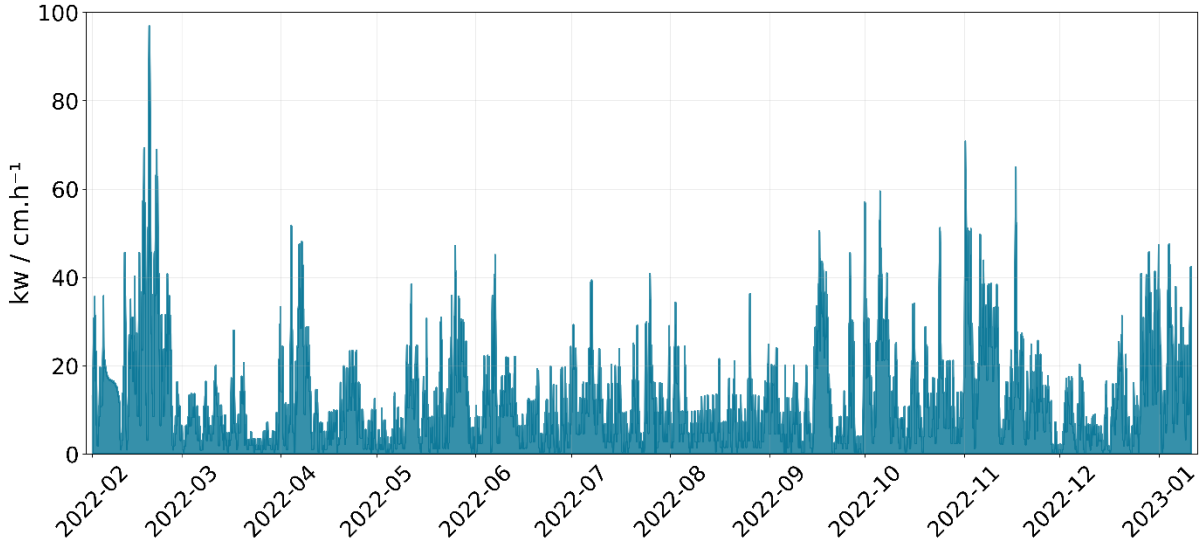

Figure S5. Time series of gas transfer velocity (k_w) at the Marsdiep jetty station from February 2022 to January 2023. k_w was calculated from local wind speed and sea surface temperature following Nightingale et al. (2000), using the pySeaFlux package v2.0.0 (Gregor and Humphreys, 2021).

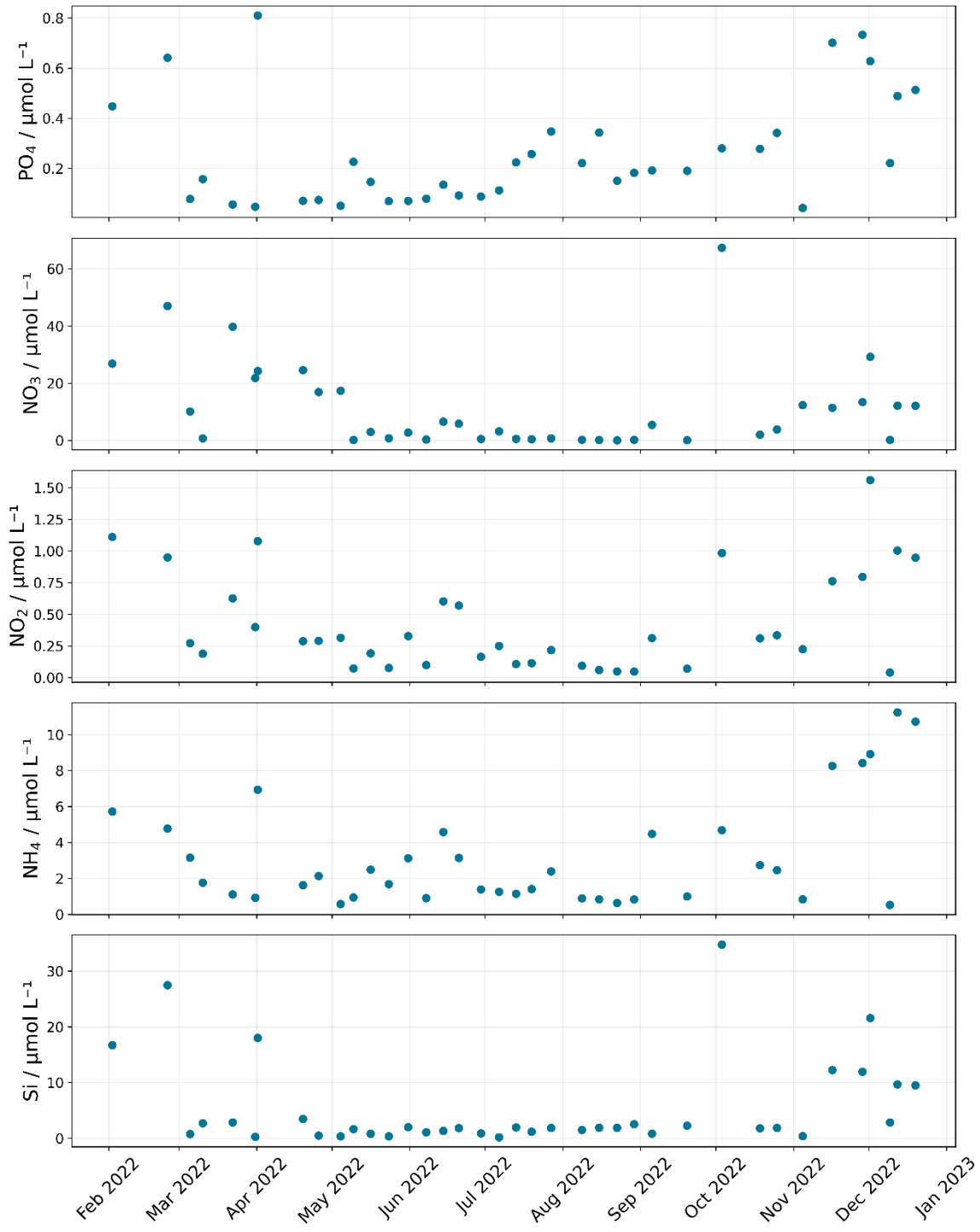

Figure S6. Seasonal variability of nutrient concentrations from February 2022-January 2023. All concentrations are in µmol L^{-1}. PO_4^{3-}: phosphate, NO_3^-: nitrate, NO_2^-: nitrite, and Si: silicate.

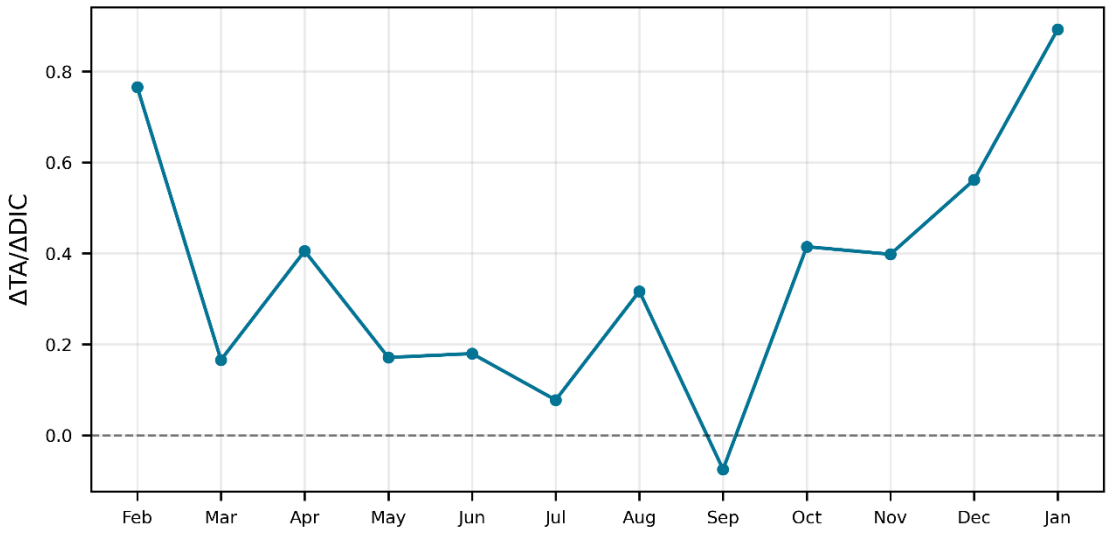

Figure S7. Monthly δTA/δDIC slopes derived from linear regressions between total alkalinity (TA) and dissolved inorganic carbon (DIC) measured at the Marsdiep tidal inlet from February 2022 to January 2023. Slopes reflect the co-variability of TA and DIC within each month. The dashed line indicates δTA/δDIC = 0.

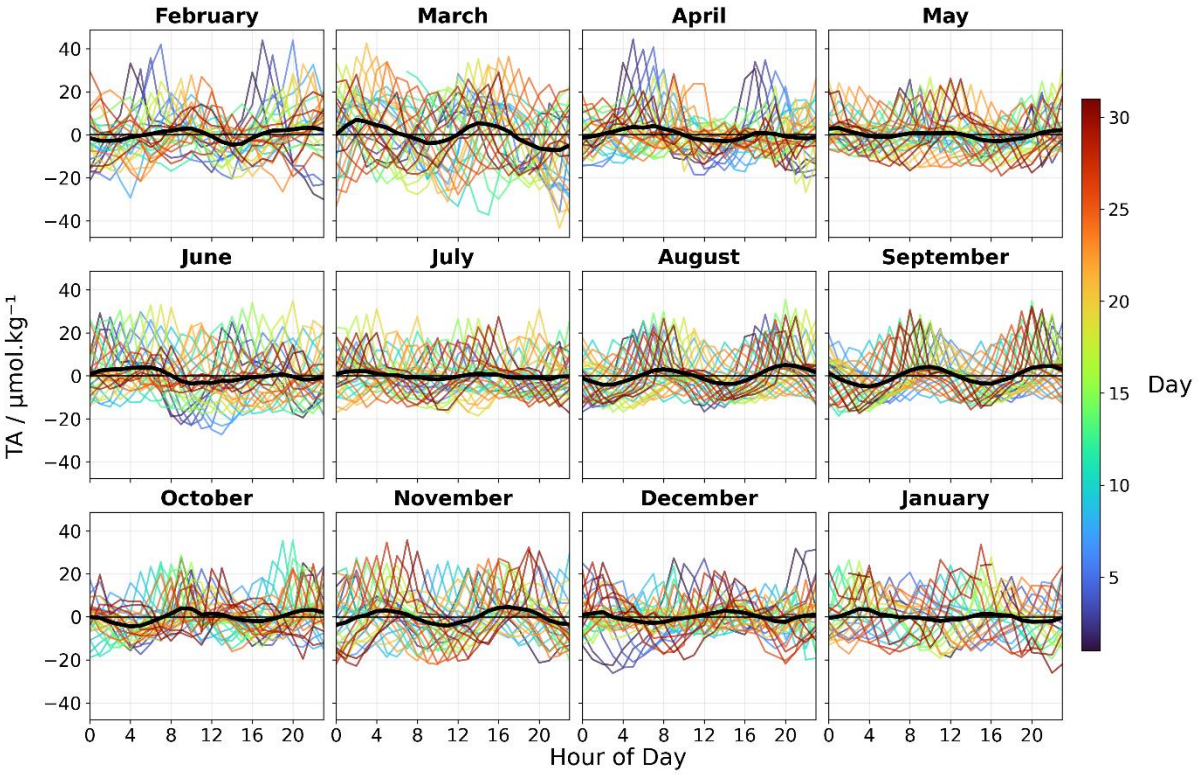

Figure S8. Seasonal diurnal variability of TA anomalies between February 2022-January 2023.

Each subplot represents a month, with the x axis showing the hour of the day (0-23). Normalised daily hourly means are plotted using a colour gradient to represent the different days of the month. Blue colours are set for the set of the month, to reach red at the end of the month. The monthly hourly mean is represented by the black line.

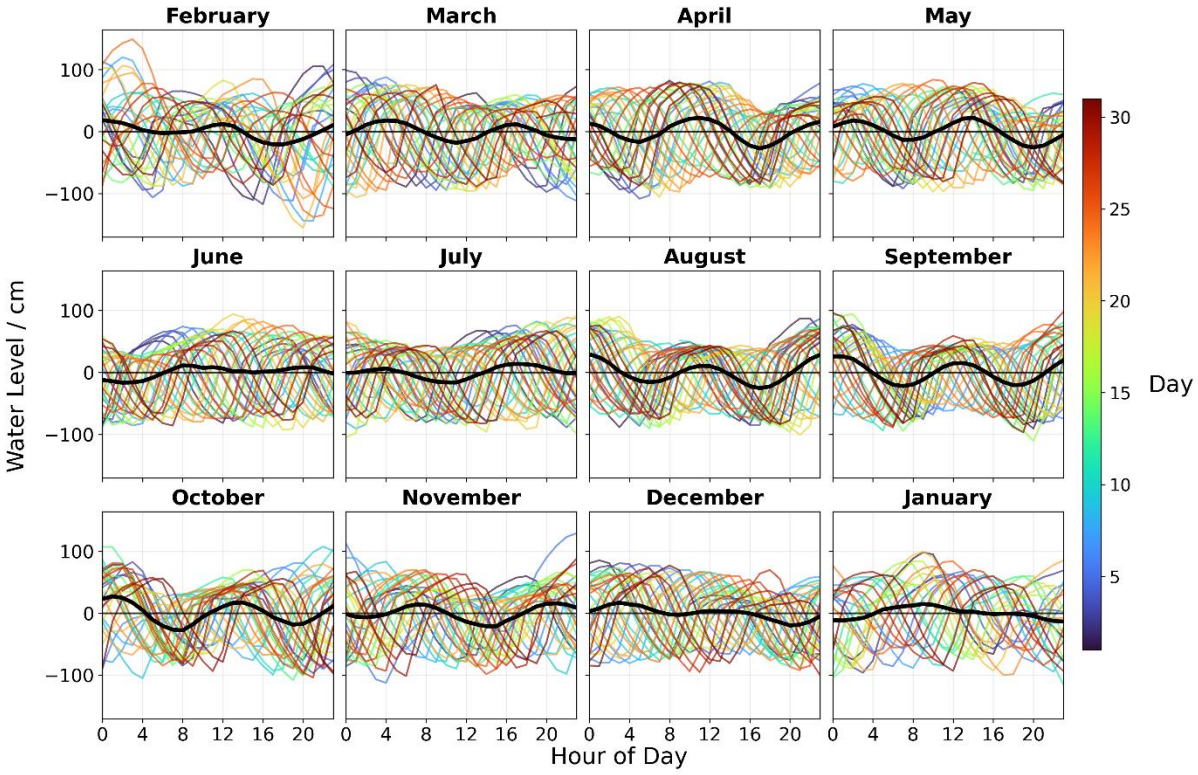

Figure S9. Seasonal diurnal variability of water level anomalies between February 2022-January 2023.

Each subplot represents a month, with the x axis showing the hour of the day (0-23). Normalised daily hourly means are plotted using a colour gradient to represent the different days of the month. Blue colours are set for the set of the month, to reach red at the end of the month. The monthly hourly mean is represented by the black line.

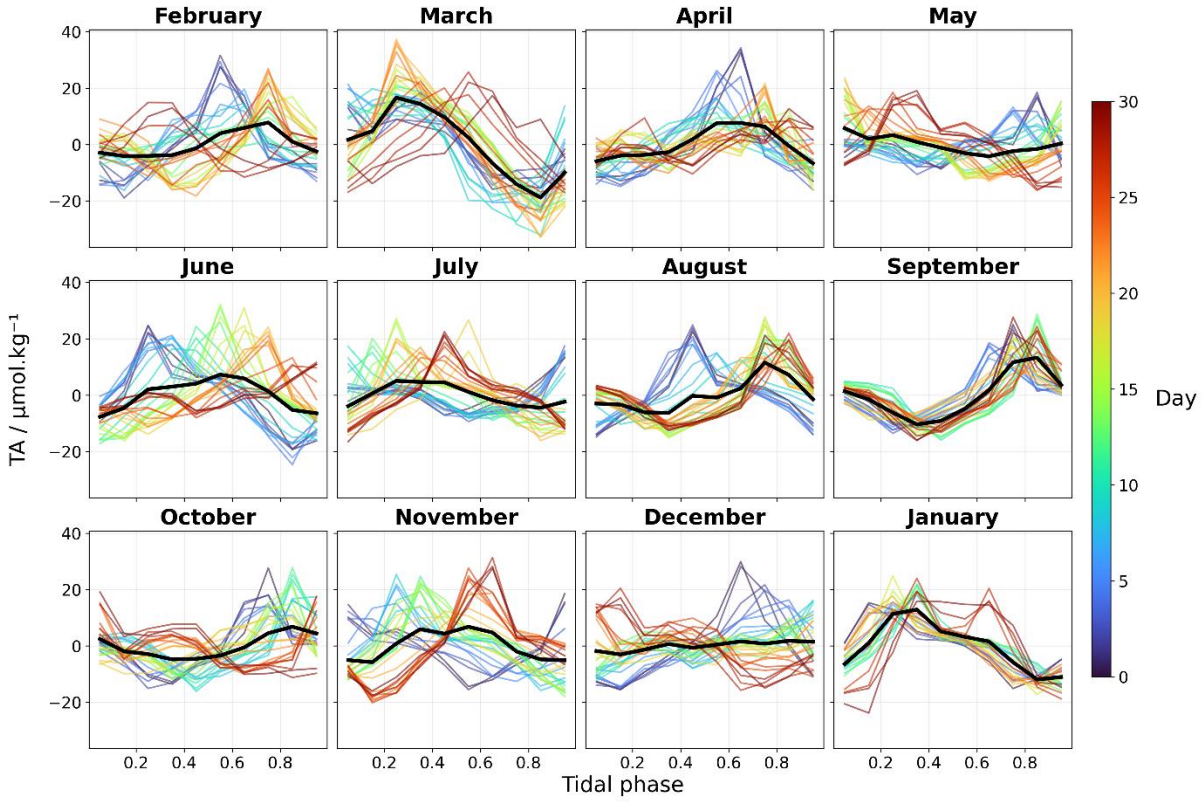

Figure S10. Tidal phase analysis variability of TA anomalies between February 2022-January 2023.

Each subplot represents a month, with the x axis showing the tidal phase (0-1), representing the normalised position within one complete tidal cycle based on the M2 tidal constituent and where 0 and 1 represent the same point in the cycle. Normalised tidal means are plotted using a colour gradient to represent the different days of the month. Blue colours are set for the start of the month, to reach red at the end of the month. The monthly tidal mean is represented by the black line.

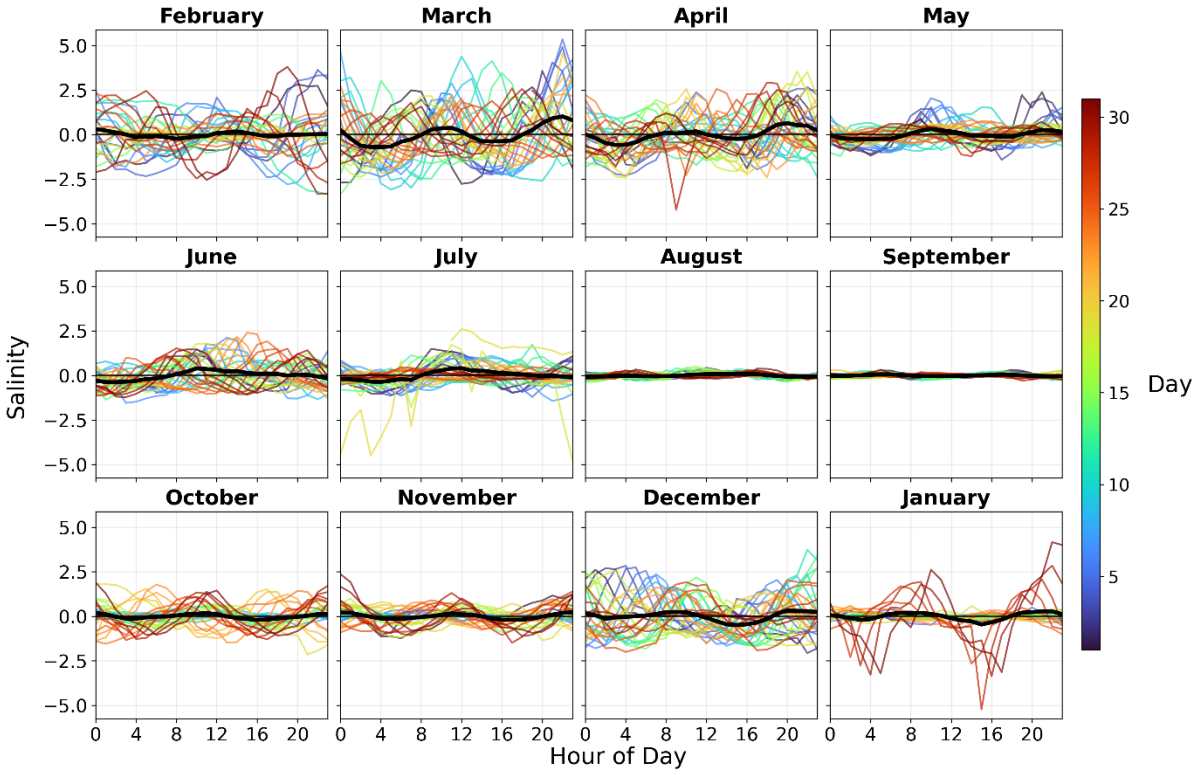

Figure S11. Seasonal diurnal variability of salinity anomalies between February 2022-January 2023.

Each subplot represents a month, with the x axis showing the hour of the day (0-23). Normalised daily hourly means are plotted using a colour gradient to represent the different days of the month. Blue colours are set for the set of the month, to reach red at the end of the month. The monthly hourly mean is represented by the black line.

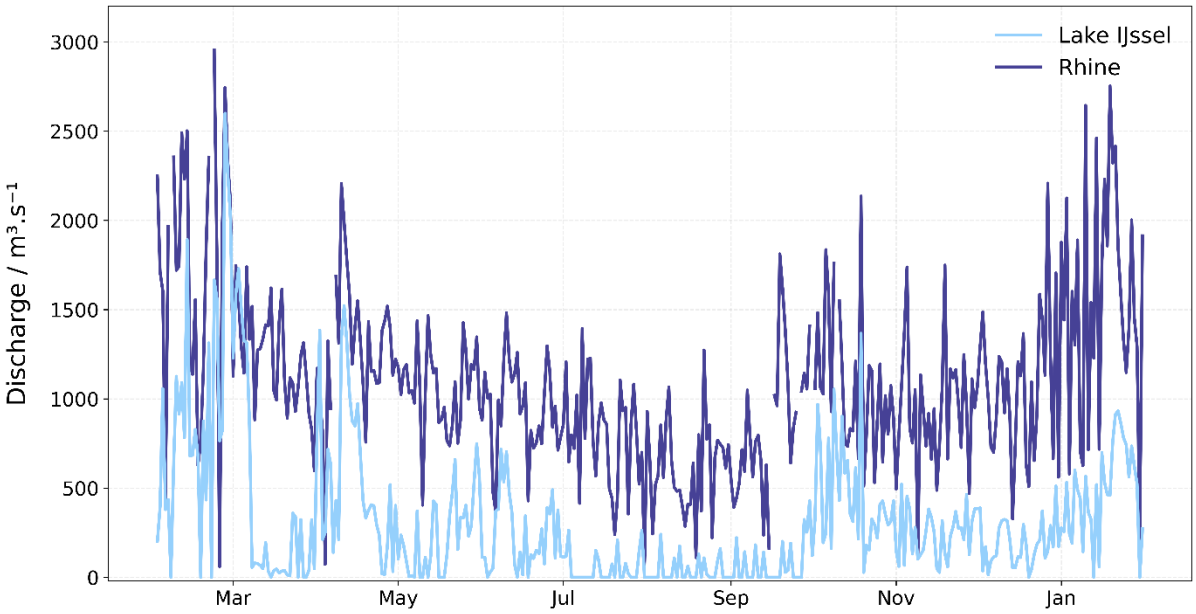

Figure S12. Daily river discharge of the Rhine River (dark blue) and Lake IJssel (light blue) for the period 2022-2023. Discharge values are given in cubic meters per second ($m^3\ s^{-1}$).

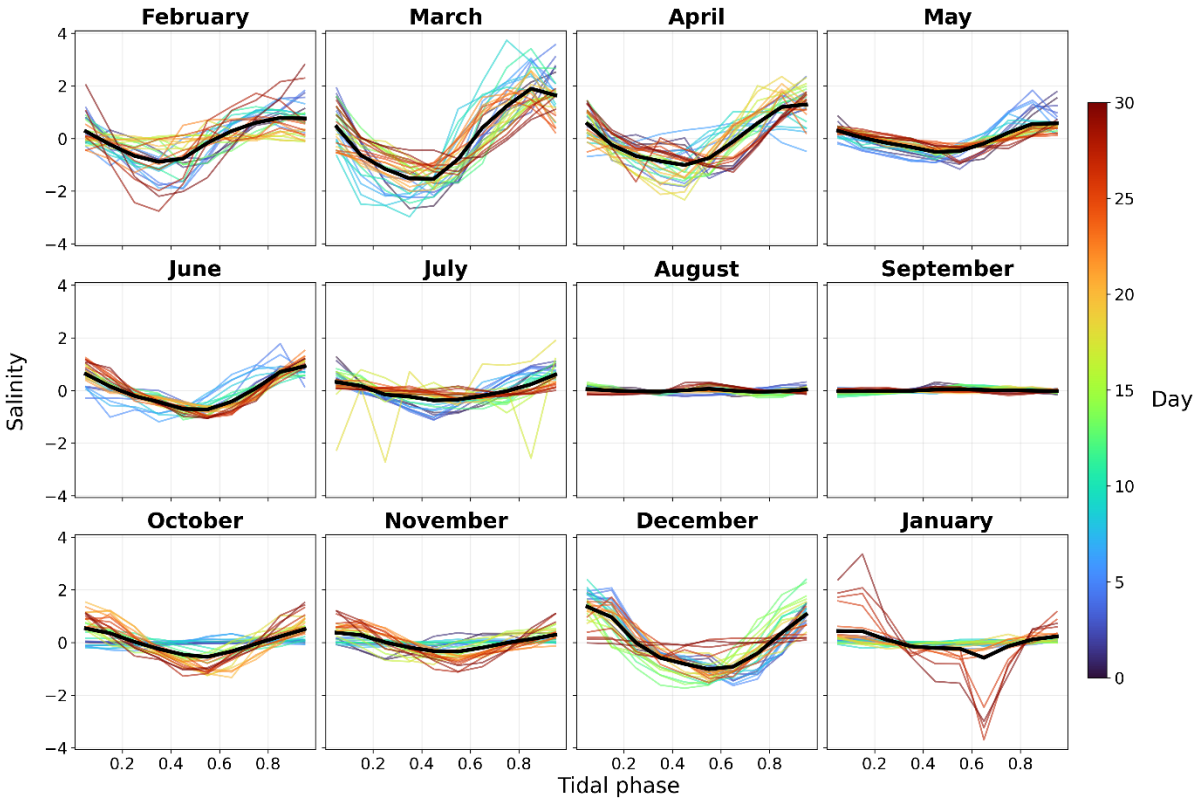

Figure S13. Tidal phase analysis variability of salinity anomalies between February 2022-January 2023.

Each subplot represents a month, with the x axis showing the tidal phase (0-1), representing the normalised position within one complete tidal cycle based on the M2 tidal constituent and where 0 and 1 represent the same point in the cycle. Normalised tidal means are plotted using a colour gradient to represent the different days of the month. Blue colours are set for the start of the month, to reach red at the end of the month. The monthly tidal mean is represented by the black line.

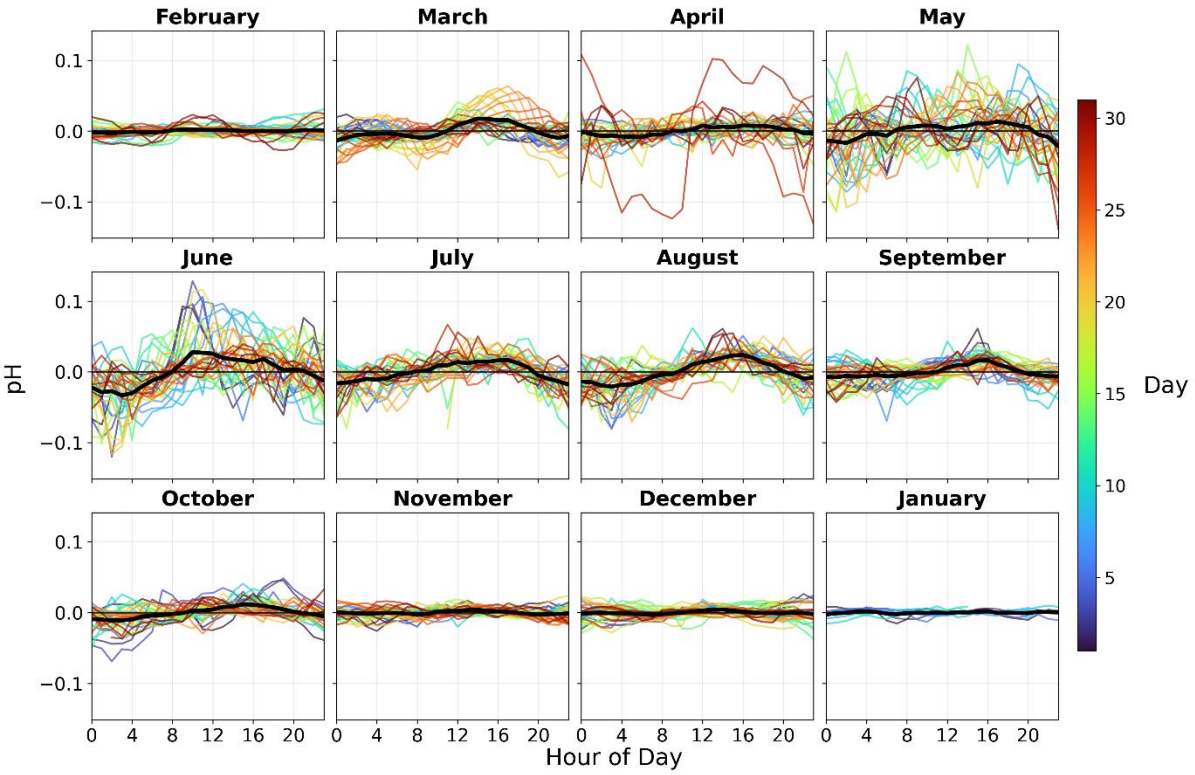

Figure S14. Seasonal diurnal variability of pH anomalies between February 2022-January 2023.

Each subplot represents a month, with the x axis showing the hour of the day (0-23). Daily hourly means are plotted using a colour gradient to represent the different days of the month. Blue colours are set for the set of the month, to reach red at the end of the month. The monthly hourly mean is represented by the black line.

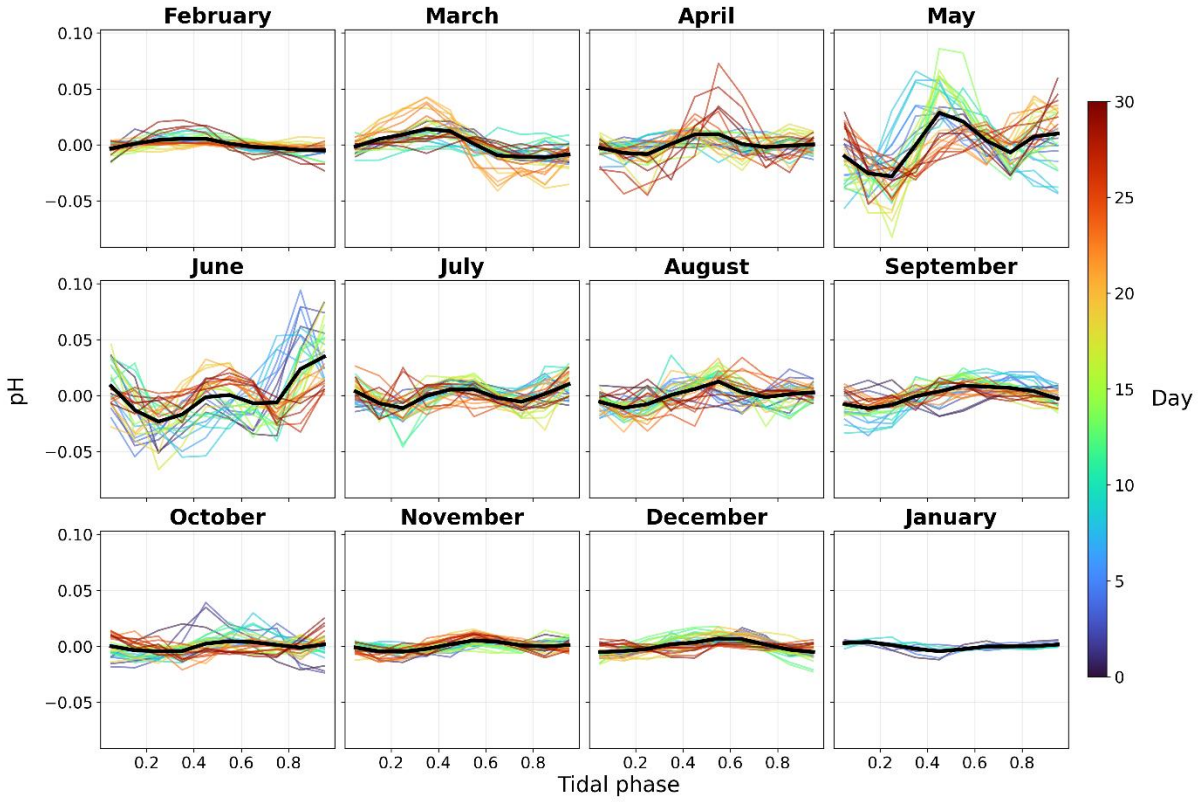

Figure S15. Tidal phase analysis variability of pH anomalies between February 2022-January 2023.

Each subplot represents a month, with the x axis showing the tidal phase (0-1), representing the normalised position within one complete tidal cycle based on the M2 tidal constituent and where 0 and 1 represent the same point in the cycle. Normalised tidal means are plotted using a colour gradient to represent the different days of the month. Blue colours are set for the start of the month, to reach red at the end of the month. The monthly tidal mean is represented by the black line.

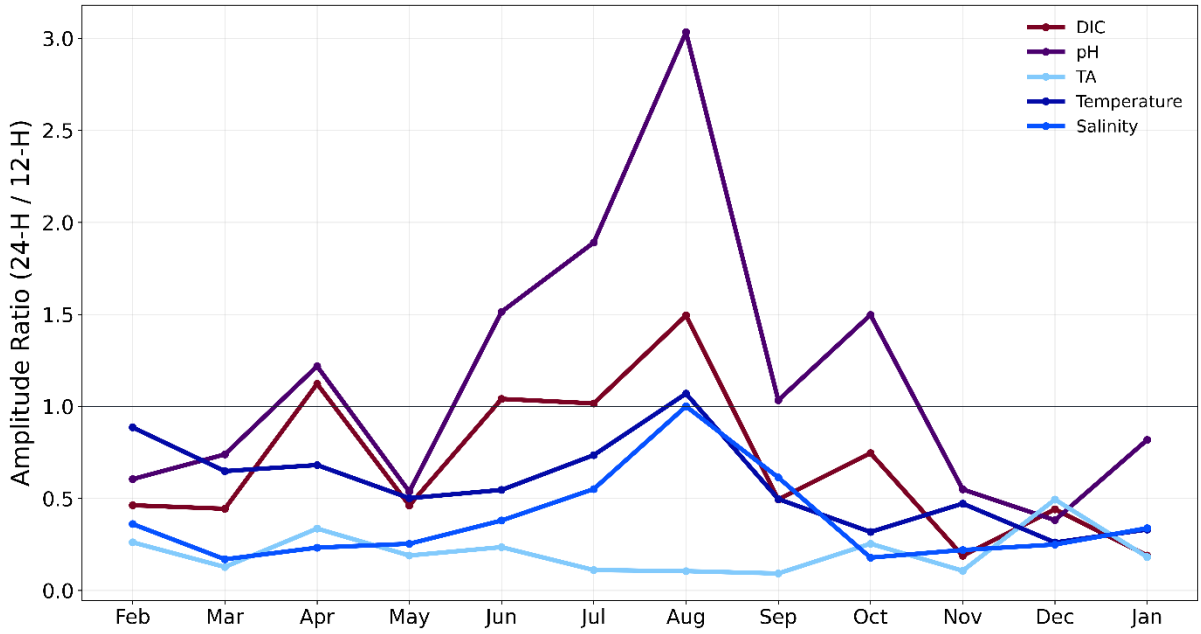

Figure S16. Fourier analysis showing amplitude ratio between the 24-H and 12-H frequencies.

The amplitude ratio is plotted for pH, TA, DIC, temperature and salinity. Values above 1 indicate a stronger diel signal, while values below 1 indicate a stronger semi-diurnal signal.

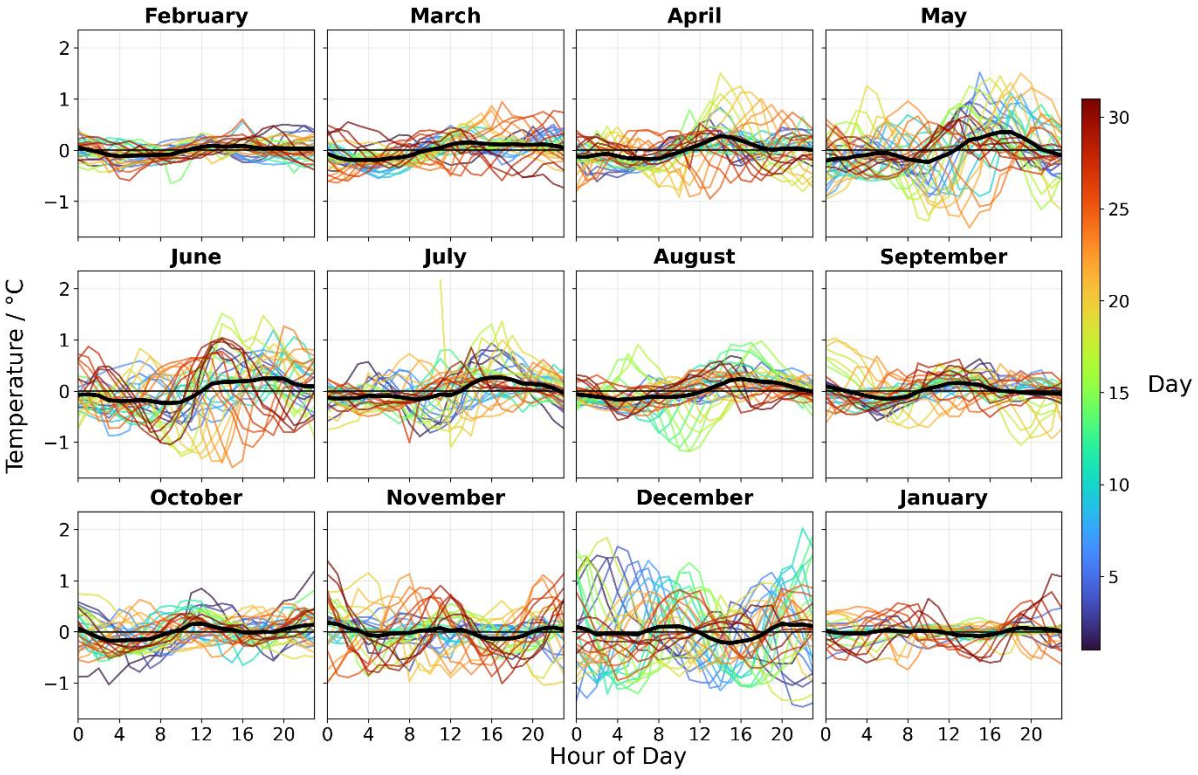

Figure S17. Seasonal diurnal variability of temperature anomalies between February 2022-January 2023.

Each subplot represents a month, with the x axis showing the hour of the day (0-23). Normalised daily hourly means are plotted using a colour gradient to represent the different days of the month. Blue colours are set for the set of the month, to reach red at the end of the month. The monthly hourly mean is represented by the black line.

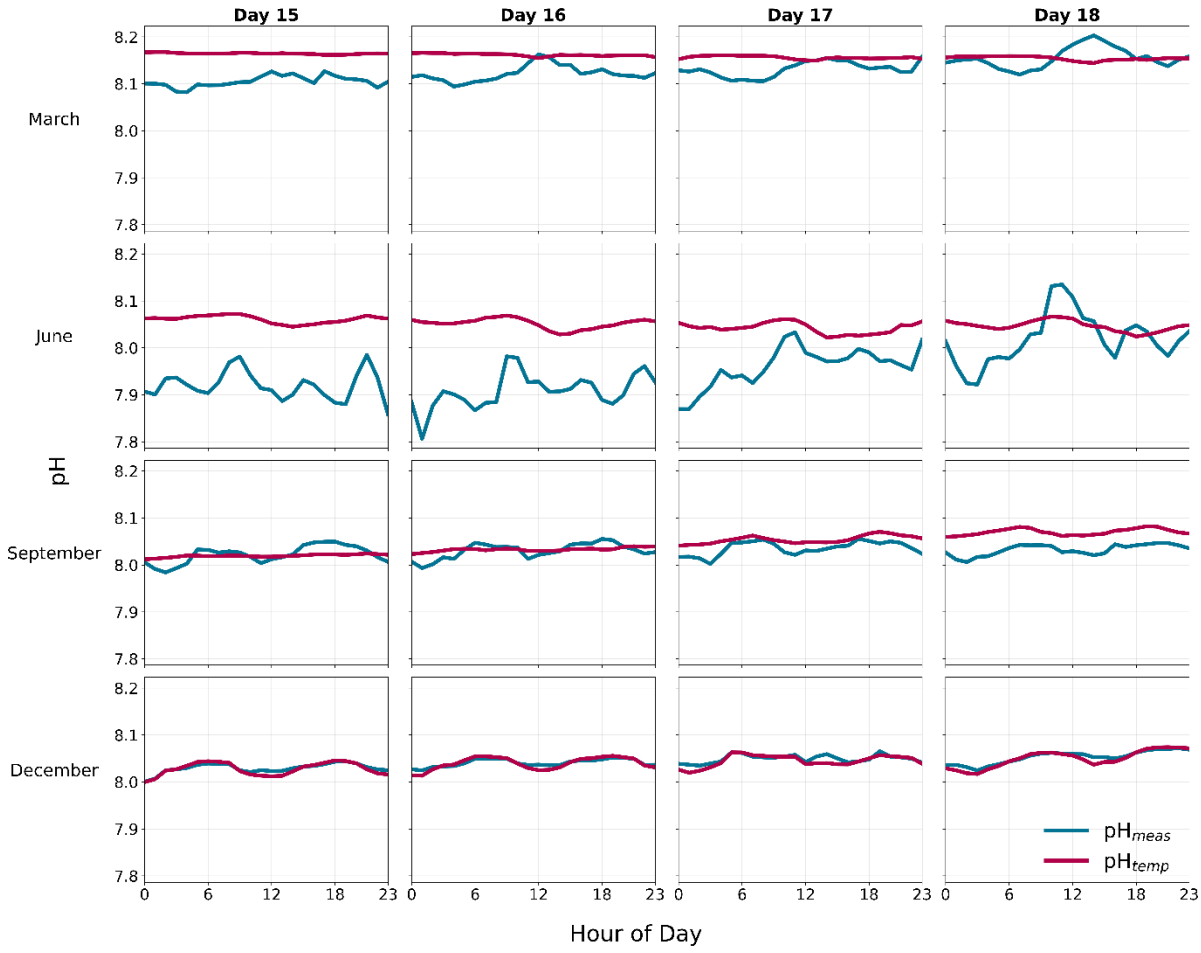

Figure S18. Comparison of pH_{meas} (blue) and pH_{temp} (red) across seasonal representative days in 2022. Four days (15-18) were selected from each month (March, June, September, December) to represent different seasonal conditions. Each subplot shows hourly mean pH values for each day.

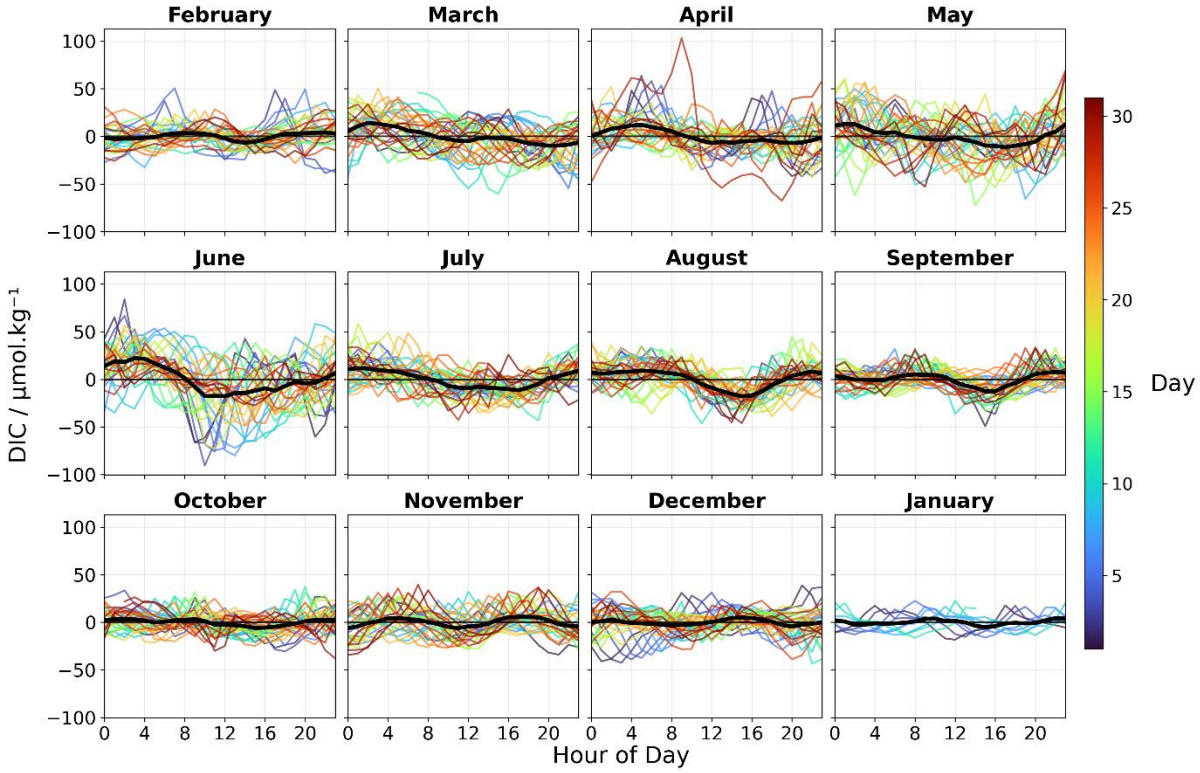

Figure S19. Seasonal diurnal variability of DIC anomalies between February 2022-January 2023.

Each subplot represents a month, with the x axis showing the tidal phase (0-1), representing the normalised position within one complete tidal cycle based on the M2 tidal constituent and where 0 and 1 represent the same point in the cycle. Normalised tidal means are plotted using a colour gradient to represent the different days of the month. Blue colours are set for the start of the month, to reach red at the end of the month. The monthly tidal mean is represented by the black line.

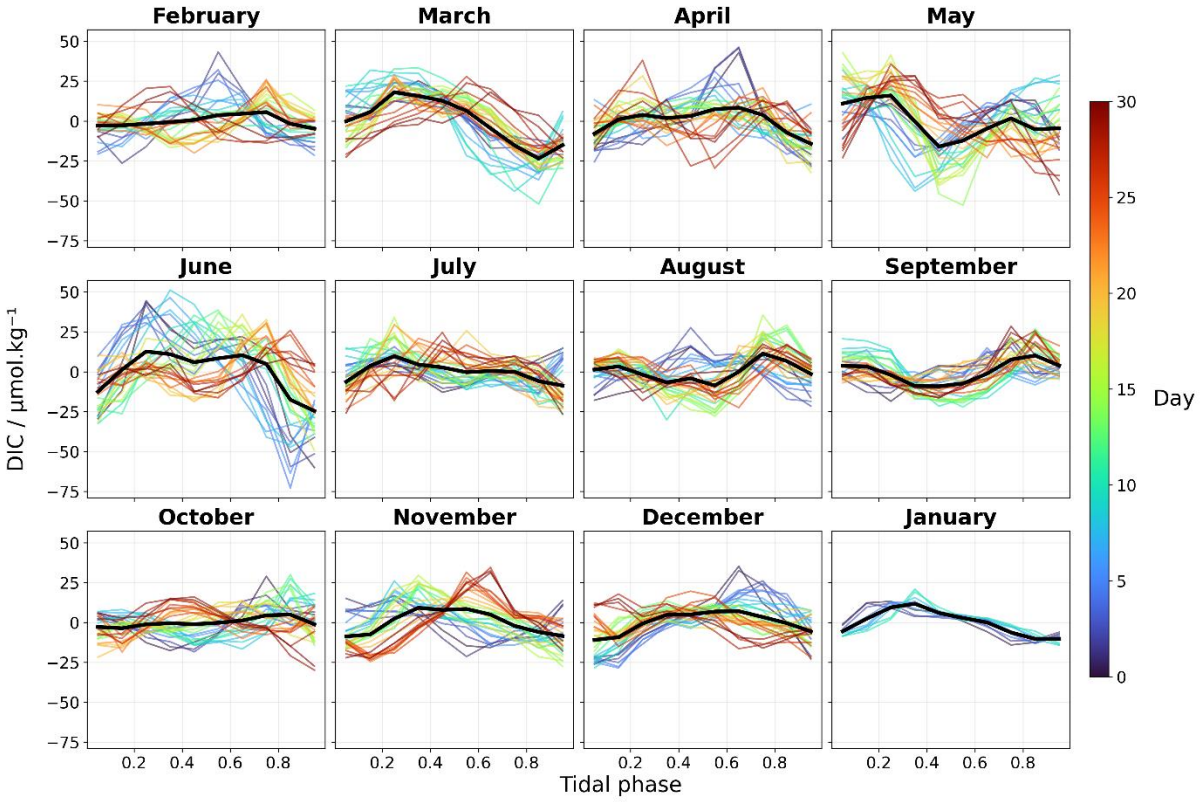

Figure S20. Tidal phase analysis variability of DIC anomalies between February 2022-January 2023.

Each subplot represents a month, with the x axis showing the tidal phase (0-1), representing the normalised position within one complete tidal cycle based on the M2 tidal constituent and where 0 and 1 represent the same point in the cycle. Normalised tidal means are plotted using a colour gradient to represent the different days of the month. Blue colours are set for the start of the month, to reach red at the end of the month. The monthly tidal mean is represented by the black line.

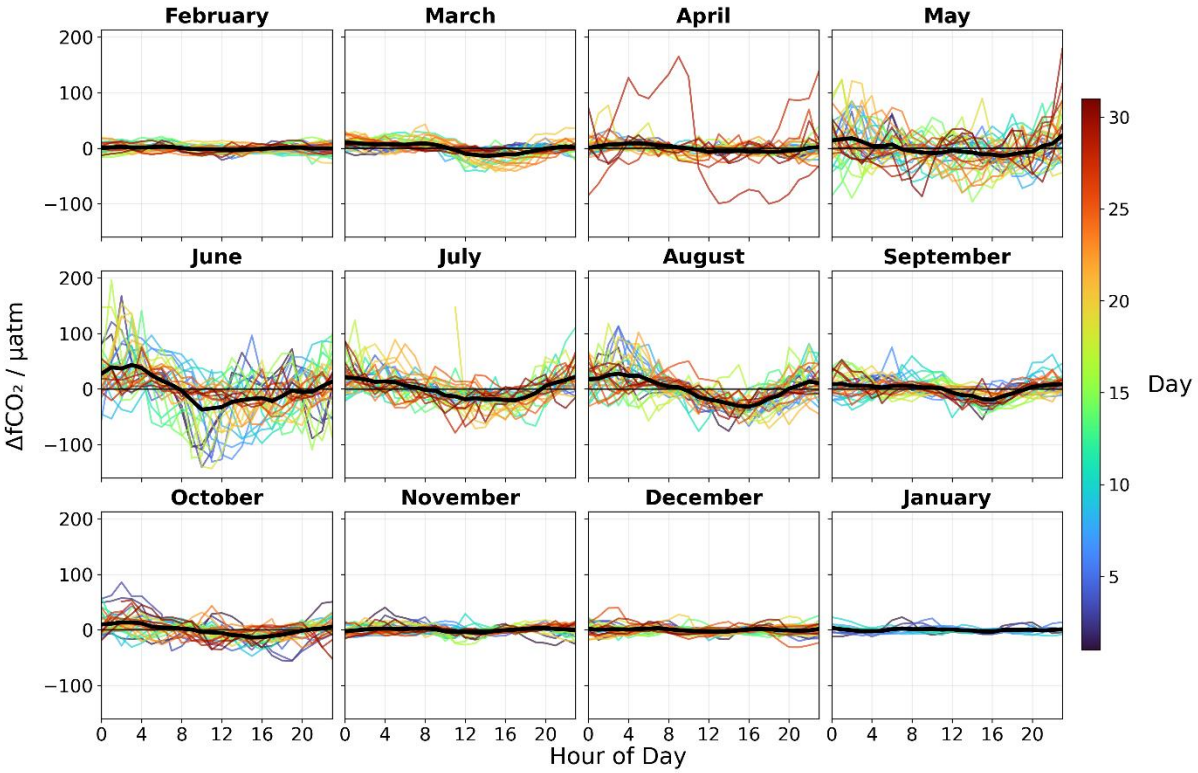

Figure S21. Seasonal diurnal variability of ΔfCO_2 anomalies between February 2022-January 2023.

Each subplot represents a month, with the x axis showing the hour of the day (0-23). Normalised daily hourly means are plotted using a colour gradient to represent the different days of the month. Blue colours are set for the set of the month, to reach red at the end of the month. The monthly hourly mean is represented by the black line.

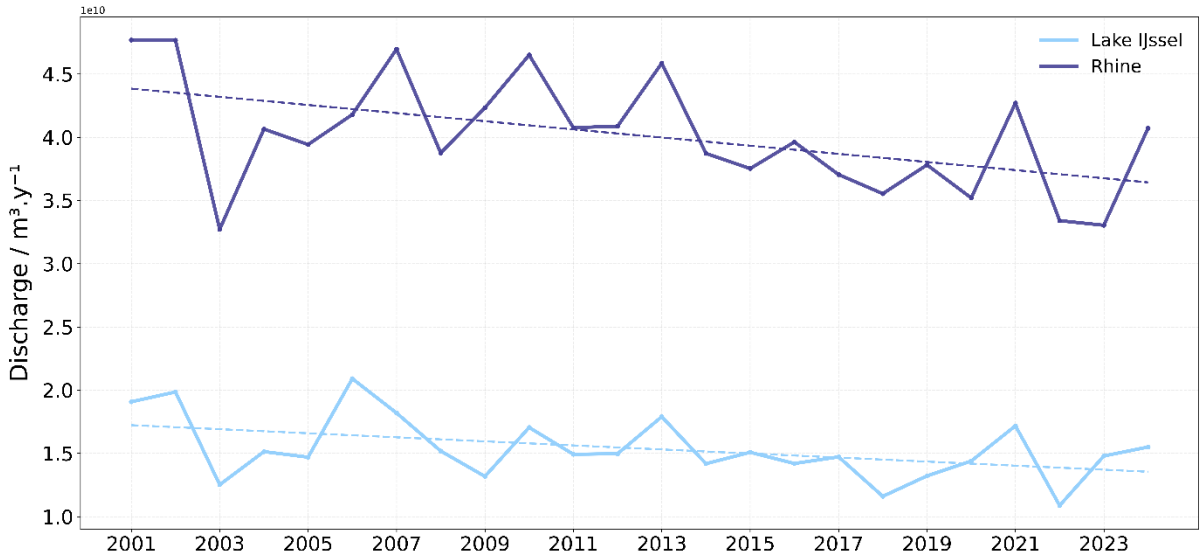

Figure S22. Yearly river discharge of the Rhine River (dark blue) and Lake IJssel (light blue) for the period 2001-2024. Discharge values are given in cubic meters per year ($m^3\ y^{-1}$).